PCCP

RSC Publishing

COMMUNICATION

View Article Online
View Journal

Enhanced ultraviolet responses in thin-film InGaP solar cells by down-shifting

Cite this: DOI: 10.1039/c3cp54096k

Received 26th August 2013,
Accepted 4th October 2013

DOI: 10.1039/c3cp54096k

www.rsc.org/pccp

Xing Sheng,†[a] Christopher J. Corcoran,†[b] Junwen He,[b] Ling Shen,[ac] Seungho Kim,[d] Jongwook Park,[d] Ralph G. Nuzzo*[ab] and John A. Rogers*[ab]

Layers of poly(methyl methacrylate) doped with the Eu complex Eu(DPEPO)(hfac)$_3$ (EuDH) provide a means for down-shifting incident ultraviolet (UV) light into the visible range, with beneficial effects on the performance of solar cells, as demonstrated with thin-film InGaP devices formed by epitaxial liftoff. Experimental and computational results establish important aspects of gain and loss mechanisms in the UV range. Measurements show that InGaP cells with coatings of EuDH doped PMMA exhibit enhanced currents (8.68 mA cm^{-2}) and power conversion efficiencies (9.48%), both due to increased responses at wavelengths between 300–360 nm.

Light management in solar cells represents an effective avenue for improving performance and reducing the overall cost of photovoltaic (PV) systems.[1] To approach efficiencies close to those defined by detailed balance limits,[2] a solar cell must have both a great electronic efficiency and a great optical efficiency. Every incident photon with an energy above the bandgap of the cell should be absorbed, and each absorption event should yield at least one electron–hole pair capable of extraction as electrical power. Historically, significant efforts have been directed toward light trapping and other schemes to enhance the absorption near the bandedge, particularly in the long wavelength side of the solar spectrum.[3–6] By contrast, less attention has been paid to the short-wavelength limit. In the ultraviolet (UV) range (300–400 nm), most PV materials naturally have high absorption coefficients, thereby eliminating the need for light trapping. Low quantum efficiencies, however, are usually obtained in this region of the spectrum, even for cells with record efficiencies.[7] Such low UV responses follow from both intrinsic and more practical considerations. First, traditional cell designs incorporate highly doped window and/or emitter layers,[8–10] which work as deadzones for UV light conversion because of the extremely short diffusion lengths for minority carriers in these regions. Second, anti-reflective coatings are typically optimized to minimize light reflections around the peak of the solar spectrum (500–700 nm), and can often have high reflection losses in the UV range.[11] Finally, in most modules, solar cells are encapsulated with glass and/or plastic covers[12] that absorb UV light. Based on our calculations, UV photons (300–400 nm) in the standard AM1.5G solar spectrum[13] have the potential to contribute a photocurrent of $\sim$1.3 mA cm^{-2}. Exploiting these UV photons efficiently can therefore improve the efficiency by a meaningful amount. Various down-shifting materials, including organolanthanide complexes, organic dyes and quantum dots, have been proposed to convert UV photons into visible ones.[14,15] Encapsulant polymer coatings doped with down-shifting materials have been demonstrated to increase UV responses and efficiencies for conventional PV cells and modules based on semiconductors like Si and CdTe.[16–20] By applying the UV down-shifting layers on top of organic solar cells, UV degradation can be mitigated and longer device lifetime can be achieved.[14] Such concepts, however, have particular potential in high efficiency III–V (GaAs, InGaP, *etc.*) solar cells, where detailed balance limits can be approached as a result of high radiation efficiencies.[21] In this paper, we demonstrate the use of a specific europium complex, Eu(DPEPO)(hfac)$_3$ [DPEPO = bis(2-(diphenylphosphino)phenyl)ether oxide, hfac = hexafluoroacetylacetonate], doped into thin films of poly(methyl methacrylate) (PMMA), as a means for down-shifting UV photons (300–360 nm) into visible photons ($\sim$610 nm). Experiments with thin-film indium gallium phosphide (InGaP) cells formed by epitaxial liftoff demonstrate improvements that result from application of such films as front side coatings. The UV gain and loss mechanisms for down-shifting are analyzed in detail by numerical simulations.

Fig. 1a presents an optical micrograph of a thin-film InGaP solar cell (500 μm × 500 μm) integrated onto a glass substrate using techniques of epitaxial liftoff and transfer printing. The materials for the cells are formed by growth on a gallium arsenide

[a] *Department of Materials Science and Engineering, University of Illinois at Urbana-Champaign, Urbana, IL 61801, USA. E-mail: jrogers@illinois.edu*
[b] *Department of Chemistry, University of Illinois at Urbana-Champaign, Urbana, IL 61801, USA. E-mail: r-nuzzo@illinois.edu*
[c] *SHU-SolarE R&D Lab, Department of Physics, Shanghai University, Shanghai 200444, P.R. China*
[d] *Department of Chemistry, The Catholic University of Korea, Yokkok, Bucheon, Kyunggi, 420-743, Korea*
† These authors contributed equally to this work.

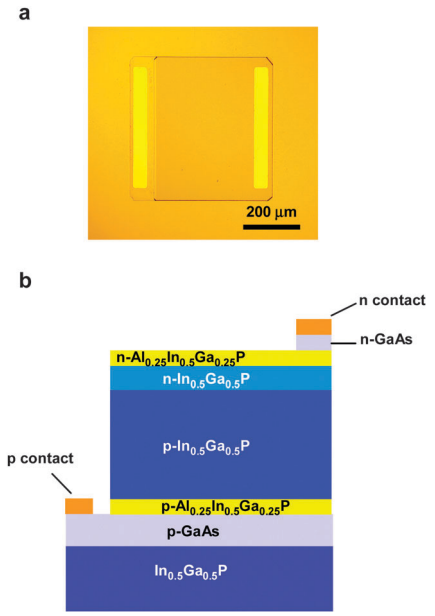

Fig. 1 (a) Optical microscope image of a thin-film InGaP cell (500 μm × 500 μm) with ohmic contacts, printed on a glass substrate. (b) Cross sectional schematic illustration of the cell, showing the InGaP homojunction, AlInGaP window layers and contacting layers.

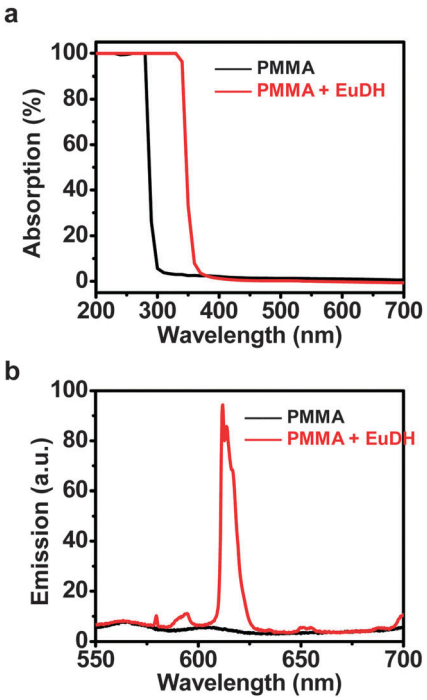

Fig. 2 Measured optical properties of a layer of PMMA layer (in black) and a layer of PMMA + EuDH (in red) on quartz substrates. The thicknesses in both cases are 40 μm. (a) Absorption spectra. (b) Emission spectra, measured with an excitation source at 365 nm.

(GaAs) substrate *via* metal–organic chemical vapor deposition (MOCVD). The detailed structure (from bottom to top) includes the GaAs substrate, a 500 nm $Al_{0.96}Ga_{0.04}As$ sacrificial layer, a 1000 nm $In_{0.5}Ga_{0.5}P$ supporting layer, a 100 nm *p*-GaAs bottom contact ($p > 1 \times 10^{19}$ cm^{-3}), a 100 nm *p*-$Al_{0.25}In_{0.5}Ga_{0.25}P$ back surface field (BSF) layer ($p = 8 \times 10^{17}$ cm^{-3}), a 1300 nm *p*-$In_{0.5}Ga_{0.5}P$ base ($p = 3 \times 10^{16}$ cm^{-3}), a 100 nm *n*-$In_{0.5}Ga_{0.5}P$ emitter ($n = 2 \times 10^{18}$ cm^{-3}), a 40 nm *n*-$Al_{0.25}In_{0.5}Ga_{0.25}P$ window layer ($n = 5 \times 10^{18}$ cm^{-3}) and a 200 nm *n*-GaAs contact ($n > 5 \times 10^{18}$ cm^{-3}). Zn and Si serve as *p*-type and *n*-type dopants, respectively. Bilayers of Cr/Au (10 nm/100 nm) form the contacts. The cells are lithographically fabricated, using H_3PO_4 (85 wt% in water)–H_2O_2 (30 wt% in water)–H_2O (1 : 13 : 12) and HCl (36 wt% in water) to etch the GaAs and InGaP/AlInGaP layers, respectively. After removing the $Al_{0.96}Ga_{0.04}As$ sacrificial layer in an ethanol-rich hydrofluoric acid (HF) solution (ethanol : HF = 1.5 : 1 by volume), individual InGaP cells can be released from the GaAs wafer and then bonded onto glass substrates by transfer printing with a flat poly(dimethylsiloxane) (PDMS) stamp.[22] A 2 μm layer of epoxy (SU-8 2002, MicroChem) acts as an adhesive to facilitate transfer. The sidewalls of the cell are encapsulated with a ~500 nm thick layer of a photocurable epoxy (SU-8 2000.5, MicroChem). Large-area metal contacts of Cr/Cu/Au (10 nm/500 nm/10 nm) are used for electrical interconnection.

The Eu(DPEPO)$(hfac)_3$ (EuDH) complex serves as the UV luminophore.[23] Powders of EuDH are mixed into a solution of PMMA (950 000 MW in anisole, 11 wt%, by MicroChem), at a concentration of 1 wt% EuDH. PMMA is an attractive choice for the polymer matrix because it is transparent at wavelengths longer than 300 nm and is commonly used for solar module encapsulation.[24] The resulting solution can be spin cast and cured at 150 °C, to remove anisole and form EuDH-doped PMMA solid films on substrates of interest. Fig. 2 shows the absorption and emission properties of a 40 μm thick PMMA + EuDH film coated on a quartz substrate, and a comparison to a 40 μm thick film without EuDH. Shown in Fig. 2a, the PMMA absorbs UV at wavelengths below ~300 nm, while the EuDH complex absorbs light between 300 nm and 360 nm. The photons absorbed by EuDH are down-shifted, with an emission peak at around 610 nm (Fig. 2b), corresponding to a Stokes shift that is much larger than that in common organic dyes.[17,19,20] The EuDH doped in a 40 μm thick PMMA film provides nearly 100% UV absorption from 300 nm to 360 nm, eliminating the need for using thick coatings as reported previously.[16–18] This thin geometry minimizes parasitic optical losses (absorption/scattering by the polymer, edge emission, *etc.*). The measured intrinsic photoluminescence quantum yield (PLQY) for the EuDH doped in PMMA is ~77%, which is one of the highest values reported in similar Eu-based complexes.[18,23]

Both PMMA and PMMA + EuDH can be coated directly on InGaP cells, as shown in Fig. 3. The PMMA (Fig. 3a) allows light ($\lambda > 300$ nm) to pass directly through, for absorption by the cell. Visible light (400–650 nm) can be absorbed by the active InGaP pn junction, to generate free carriers. Most of the UV light (300–400 nm), however, is blocked by the 40 nm thick AlInGaP window layer, due to the high absorption coefficient of AlInGaP in the UV range.[25] As a result, low UV responses are observed; similar behaviors are also reported in GaAs and InGaP cells

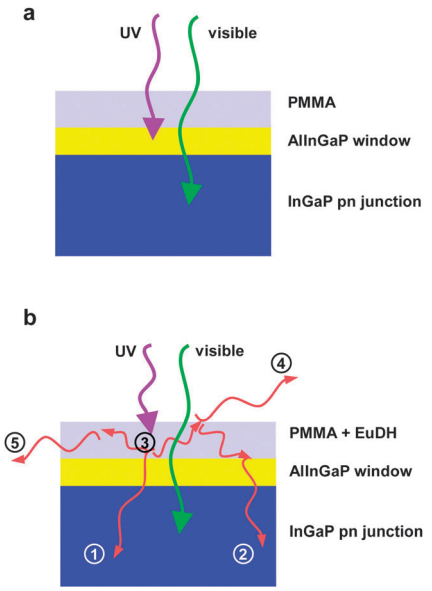

Fig. 3 Cross sectional schematic illustrations of light responses for InGaP cells with different coatings: (a) a PMMA layer and (b) a PMMA + EuDH layer.

with or close to record efficiencies,[7,9,10] for similar reasons. With PMMA + EuDH (Fig. 3b), UV light from 300 nm to 360 nm is absorbed by the EuDH and down-shifted, without affecting light at longer wavelengths ($\lambda > 360$ nm). The down-shifted light has an isotropic emission profile; it can directly penetrate into the high-index InGaP cell (process 1), or undergo total internal reflection (TIR) at the PMMA/air interface and then couple into the InGaP cell (process 2). Both mechanisms contribute to carrier generation, thereby improving the UV responses. Various loss mechanisms are also present due to non-unity down-shift efficiency (PLQY = 77%) (process 3), out-coupling into the air due to non-TIR at the PMMA/air interface (process 4), and light escaping at the edges of the device (process 5).

To predict and compare the performance of the two device configurations in Fig. 3, numerical simulations are employed to determine the external quantum efficiency (EQE) spectra, plotted in Fig. 4a. The EQE can be written

$$\mathrm{EQE}(\lambda) = \mathrm{IQE}(\lambda)\cdot[1 - R(\lambda)] \quad (1)$$

where the internal quantum efficiency (IQE) spectra can be calculated through electrical modeling[26] of the 1D InGaP cell structure shown in Fig. 1b. The reflection spectra $R(\lambda)$ can be calculated by combining Fresnel reflections and ray tracing.[27] Optical and electrical properties of different layers are found in the literature.[25,28,29] The InGaP cell with a PMMA coating shows a low UV response because of high absorption introduced by the AlInGaP window layer, as discussed in Fig. 3a. In the visible range, the EQE peaks at around 600 nm and decreases to zero at the band-edge of InGaP ($E_g \sim 1.9$ eV). If the PMMA layer is doped with EuDH, most of the UV light from 300 nm to 360 nm is absorbed by the EuDH and down-shifted into photons with wavelengths of ~610 nm, where the InGaP cell has its maximum IQE. In this case, the EQE can be estimated by

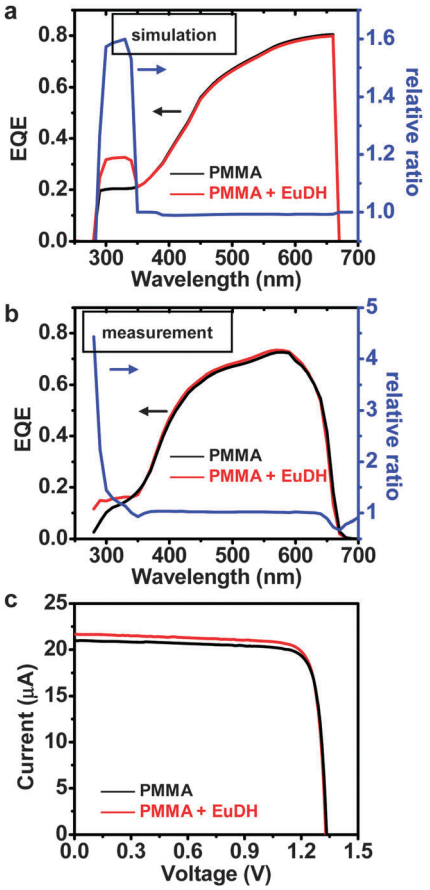

Fig. 4 Performance of InGaP cells coated with PMMA (in black) and PMMA + EuDH (in red): (a) simulated EQE spectra and the relative ratio; (b) measured EQE spectra and the relative ratio; (c) measured current–voltage characteristics. The relative ratios between black and red curves are also indicated in (a) and (b).

$$\begin{aligned}&\mathrm{EQE}(\lambda = 300\text{–}360\ \mathrm{nm})\\ &= \mathrm{IQE}(\lambda = 610\ \mathrm{nm})\cdot[1 - R_{\mathrm{air/PMMA}}]\cdot\mathrm{PLQY}\cdot[1 - \mathrm{escaped\ light}]\\ &= 90\%\cdot(1\text{–}4\%)\cdot 77\%\cdot(1\text{–}50\%)\\ &= 33\% \quad (2)\end{aligned}$$

Despite the various loss mechanisms for the luminescent photons, a significant fraction of photons are collected by the InGaP cell, resulting in an improved response from 300 nm to 360 nm. The EQE at longer wavelengths ($\lambda > 360$ nm) is unaffected due to the transparency of the PMMA + EuDH in this range.

Fig. 4b presents the measured EQE spectra of InGaP cells with PMMA and PMMA + EuDH coatings. In agreement with simulation results shown in Fig. 4a, the cell with PMMA + EuDH exhibits an improved EQE from 280 nm to 360 nm compared to the cell with a PMMA coating. The EQE spectra from 360 nm to 700 nm for both cells are identical. The differences between simulation and experimental results (Fig. 4a and b) likely arise from differences between the optical properties of InGaP and AlInGaP used in simulations and the experimental values and from loss mechanisms associated scattering and other parasitics. Fig. 4c shows the measured current–voltage characteristics of the two cells under the standard AM1.5G spectrum.

Improved UV responses associated with EuDH down-shifting increases the current density from 8.40 mA cm^{-2} to 8.68 mA cm^{-2}, with a relative increase of about 3.5%. For the cells with PMMA and with PMMA + EuDH, the efficiencies are 9.28% and 9.48%, respectively. (In these comparisons, we use pairs of cells that exhibited nearly identical performance, as measured before applying the coatings.)

In conclusion, we demonstrated that PMMA coatings doped with a luminescent material, EuDH, can improve the UV responses of thin-film InGaP cells by light down-shifting. As PMMA is a commonly used encapsulation material, this luminescent layer can be readily adopted for current commercial solar modules without altering the active cell structure design. Further performance improvements can be achieved by addressing the various loss mechanisms mentioned in Fig. 3b. For example, development of luminophores with increased luminescence efficiency (PLQY > 80%) and expanded absorption range (*e.g.* from 300 nm to 450 nm) with little cross-coupling and a similar Stokes shift could be valuable. In addition, conversion of UV photons into multiple visible or infrared photons *via* multi-exciton generation offers potential for quantum efficiencies larger than 100%.[30,31] From the standpoint of optical design, light that escapes from the edges of the device can be collected using luminescent concentrators.[27] To reduce the coupling loss, photonic/plasmonic structures and dyes/quantum dots with controlled anisotropic emission can be considered. Similar designs can be employed directly with world-record Si and GaAs cells,[7] although the relative increases in efficiency will be less than those observed with InGaP cells, due to higher overall photocurrents in these systems. Nevertheless, the approaches described here are notable for their ability to be used, in a simple additive fashion, with advanced cell designs and other optical management techniques.

Acknowledgements

This work is supported by the DOE 'Light-Material Interactions in Energy Conversion' Energy Frontier Research Center under grant DE-SC0001293. L. Shen acknowledges support from China Scholarship Council. S. Kim and J. Park are supported by the National Research Foundation of Korea (NRF) grant funded by the Korea government (MEST) (No. 2012001846). We thank Prof. N. C. Giebink for PLQY measurements.

References

1 A. Polman and H. A. Atwater, *Nat. Mater.*, 2012, **11**, 174.
2 W. Shockley and H. A. Queisser, *J. Appl. Phys.*, 1961, **32**, 510.
3 X. Sheng, L. Z. Broderick and L. C. Kimerling, *Opt. Commun.*, 2013, DOI: 10.1016/j.optcom.2013.07.085.
4 Z. Yu, A. Raman and S. Fan, *Proc. Natl. Acad. Sci. U. S. A.*, 2010, **107**, 17491.
5 H. A. Atwater and A. Polman, *Nat. Mater.*, 2010, **9**, 205.
6 E. Yablonovitch, *J. Opt. Soc. Am.*, 1980, **70**, 1362.
7 M. A. Green, K. Emery, Y. Hishikawa, W. Warta and E. D. Dunlop, *Prog. Photovoltaics*, 2013, **21**, 827.
8 J. Zhao, A. Wang and M. A. Green, *Prog. Photovoltaics*, 1999, **7**, 471.
9 M. A. Steiner, J. F. Geisz, I. Garcia, D. J. Friedman, A. Duda and S. R. Kurtz, *J. Appl. Phys.*, 2013, **113**, 123109.
10 J. F. Geisz, M. A. Steiner, I. García, S. R. Kurtz and D. J. Friedman, *Appl. Phys. Lett.*, 2013, **103**, 041118.
11 J. Zhao and M. A. Green, *IEEE Trans. Electron Devices*, 1991, **38**, 1925.
12 F. J. Pern and A. W. Czanderna, *Sol. Energy Mater. Sol. Cells*, 1992, **25**, 3.
13 ASTMG173-03, Standard Tables for Reference Solar Spectral Irradiances: Direct Normal and Hemispherical on 37 degree Tilted Surface (ASTM International, West Conshohocken, Pennsylvania, 2005).
14 E. Klampaftis, D. Ross, K. R. McIntosh and B. S. Richards, *Sol. Energy Mater. Sol. Cells*, 2009, **93**, 1182.
15 X. Huang, S. Han, W. Huang and X. Liu, *Chem. Soc. Rev.*, 2013, **42**, 173.
16 A. Le Donne, M. Acciarri, D. Narducci, S. Marchionna and S. Binetti, *Prog. Photovoltaics*, 2009, **17**, 519.
17 K. R. McIntosh, G. Lau, J. N. Cotsell, K. Hanton, D. L. Batzner, F. Bettiol and B. S. Richards, *Prog. Photovoltaics*, 2009, **17**, 191.
18 J. Liu, K. Wang, W. Zheng, W. Huang, C. H. Li and X. Z. You, *Prog. Photovoltaics*, 2013, **21**, 668.
19 L. Danos, T. Parel, T. Markvart, V. Barrioz, W. S. M. Brooks and S. J. C. Irvine, *Sol. Energy Mater. Sol. Cells*, 2012, **98**, 486.
20 Y. Li, Z. Li, Y. Wang, A. Compaan, T. Ren and W. Dong, *Energy Environ. Sci.*, 2013, **6**, 2907.
21 O. D. Miller and E. Yablonovitch, *IEEE J. Photovolt.*, 2012, **2**, 303.
22 J. Yoon, S. Jo, I. S. Chun, I. Jung, H. Kim, M. Meitl, E. Menard, X. Li, J. J. Coleman, U. Paik and J. A. Rogers, *Nature*, 2010, **465**, 329.
23 O. Moudam, B. C. Rowan, M. Alamiry, P. Richardson, B. S. Richards, A. C. Jones and N. Robertson, *Chem. Commun.*, 2009, 6649.
24 N. D. Kaushika and K. Sumathy, *Renewable Sustainable Energy Rev.*, 2003, **7**, 317.
25 H. Kato, S. Adachi, H. Nakanishi and K. Ohtsuka, *Jpn. J. Appl. Phys.*, 1994, **33**, 186.
26 Y. Liu, Y. Sun and A. Rockett, *Sol. Energy Mater. Sol. Cells*, 2012, **98**, 124.
27 X. Sheng, L. Shen, T. Kim, L. Li, X. Wang, R. Dowdy, P. Froeter, K. Shigeta, X. Li, R. G. Nuzzo, N. C. Giebink and J. A. Rogers, *Adv. Energy Mater.*, 2013, **3**, 991.
28 E. Palik, *Handbook of optical constants of solids*, Academic Press, 1998.
29 http://www.ioffe.ru/SVA/NSM/Semicond/.
30 B. S. Richards, *Sol. Energy Mater. Sol. Cells*, 2006, **90**, 1189.
31 V. Sukhovatkin, S. Hinds, L. Brzozowski and E. H. Sargent, *Science*, 2009, **324**, 1542.

